A&A 527, A63 (2011)
DOI: 10.1051/0004-6361/201015371

Astronomy & Astrophysics

The HARPS search for southern extra-solar planets

XXVII. Seven new planetary systems⋆,⋆⋆

C. Moutou[1], M. Mayor[2], G. Lo Curto[3], D. Ségransan[2], S. Udry[2], F. Bouchy[4,5], W. Benz[6], C. Lovis[2], D. Naef[2], F. Pepe[2], D. Queloz[2], N.C. Santos[7], and S. G. Sousa[7]

[1] Laboratoire d'Astrophysique de Marseille, OAMP, Université Aix-Marseille & CNRS, 38 rue Frédéric Joliot-Curie, 13388 Marseille Cedex 13, France
e-mail: Claire.Moutou@oamp.fr
[2] Observatoire de Genève, Université de Genève, 51 Ch. des Maillettes, 1290 Sauverny, Switzerland
[3] ESO, Karl-Schwarzschild Strasse, 2, Garching bei München, Germany
[4] Institut d'Astrophysique de Paris, 98bis bd Arago, 75014 Paris, France
[5] Observatoire de Haute Provence, OAMP, CNRS, 06670 Saint Michel l'Observatoire, France
[6] Physikalisches Institut Universität Bern, Sidlerstrasse 5, 3012 Bern, Switzerland
[7] Centro de Astrofisica e Departamento de Fisica e Astronomia, Universidade do Porto, Rua das Estrelas, 4150-762 Porto, Portugal

Received 9 July 2010 / Accepted 7 December 2010

ABSTRACT

We are conducting a planet search survey with HARPS since seven years. The volume-limited stellar sample includes all F2 to M0 main-sequence stars within 57.5 pc, where extrasolar planetary signatures are systematically searched for with the radial-velocity technics. In this paper, we report the discovery of new substellar companions of seven main-sequence stars and one giant star, detected through multiple Doppler measurements with the instrument HARPS installed on the ESO 3.6 m telescope, La Silla, Chile. These extrasolar planets orbit the stars HD 1690, HD 25171, HD 33473A, HD 89839, HD 113538, HD 167677, and HD 217786. The already-published giant planet around HD 72659 is also analysed here, and its elements are better determined by the addition of HARPS and Keck data. The other discoveries are giant planets in distant orbits, ranging from 0.3 to 29 $M_{\rm Jup}$ in mass and between 0.7 and 10 years in orbital period. The low metallicity of most of these new planet-hosting stars reinforces the current trend for long-distance planets around metal-poor stars.
Long-term radial-velocity surveys allow probing the outskirts of extrasolar planetary systems, although confidence in the solution may be low until more than one orbital period is fully covered by the observations. For many systems discussed in this paper, longer baselines are necessary to refine the radial-velocity fit and derive planetary parameters. The radial-velocity time series of stars BD -114672 and HIP 21934 are also analysed and their behaviour interpreted in terms of the activity cycle of the star, rather than long-period planetary companions.

Key words. planets and satellites: detection – techniques: radial velocities

1. Introduction

The complementarity between planet search techniques will allow us in a mid-future to draw the general picture of extrasolar systems. The transit method is strongly biased towards short-period planets, while direct imaging will be limited to exploring the outer regions of close-by systems. Intermediately, the radial-velocity surveys, conducted for more than 15 years, are continuously discovering planets in the wide period range between 1 day and 15 years. In some more years, we will be able to study the same extrasolar systems by means of the gravitational perturbation inferred by the planets on their star (by the radial-velocity and/or the astrometric technics), and direct imaging with the aid of the next-generation high-contrast instruments. This will be possible only for a few nearby systems that contain outer giant planets, or for young systems when the planet has a higher self-luminosity than a planet of similar mass in an evolved system. The combination of both methods will permit calibrating the atmospheric models, i.e., the relationship between the mass of the planet and its spectral energy distribution (e.g., Baraffe et al. 2003; Fortney et al. 2008).

In this context, the volume-limited sample conducted with HARPS since 2003 is one of the main sources of favourable targets for future direct imaging surveys. With a precision of about 2 m/s over 850 stars, it has allowed the discovery of 32 planets so far (Pepe et al. 2004; Moutou et al. 2005; Lo Curto et al. 2006; Naef et al. 2007; Moutou et al. 2009; Lo Curto et al. 2010; Ségransan et al. 2010; Naef et al. 2010). In this paper, we present the HARPS data collected for eleven stars in this stellar sample, which gathers F2 to M0 main-sequence stars closer than 57.5 pc from the Sun. Their radial-velocity variations is analysed and interpreted as the signature of planetary companions, except in two cases where we show strong evidence for the detection of the stellar long-term magnetic cycle. In Sect. 2, the parent stars are

⋆ Based on observations made with the HARPS instrument on the ESO 3.6 m telescope at La Silla Observatory under programme IDs 072.C-0488(E) and 085.C-0019.

⋆⋆ RV data are only available in electronic form at the CDS via anonymous ftp to cdsarc.u-strasbg.fr (130.79.128.5) or via http://cdsarc.u-strasbg.fr/viz-bin/qcat?J/A+A/527/A63

described, while radial-velocity observations and their analysis are presented in Sect. 3; a discussion follows in Sect. 4.

2. Characteristics of the host stars

The spectroscopic analysis of the stars has been conducted on the combined HARPS spectra, following the method described in Sousa et al. (2008). The method is based on the equivalent widths of Fe I and Fe II weak lines, by imposing excitation and ionization equilibrium assuming LTE. For this task the 2002 version of the code MOOG was used (Sneden 1973) and a grid of Kurucz Atlas 9 plane-parallel model atmospheres (Kurucz 1993). Equivalent widths of spectral lines are estimated with the ARES code (Sousa et al. 2007), from which the values of $T_{\rm eff}$, $\log g$ and [Fe/H] are derived. Actual errors on these parameters are obtained by quadratically adding 60 K, 0.1 and 0.04 dex respectively to the internal errors on $T_{\rm eff}$, $\log g$ and [Fe/H]. These values were estimated by considering the typical dispersion in each parameter comparison plot with the infra-red flux method (Casagrande et al. 2006), presented in Figs. 3 to 5 of Sousa et al. (2008). The stellar luminosity was calculated based on Hipparcos photometry (ESA 1997) and revised Hipparcos parallaxes (van Leeuwen 2007), including the bolometric correction as calibrated in Flower (1996). Theoretical evolutionary tracks are compared with the measured values to estimate the mass, radius and age of the stars with a Bayesian analysis[1] (da Silva et al. 2006). The width and contrast of the cross-correlation function are measured to estimate the projected rotational velocity of the star. Finally, the activity indicator $\log R'_{\rm HK}$ is measured on individual spectra when the flux is sufficient at 390 nm (Santos et al. 2002).

Tables 1 summarize the measured and derived parameters of the stars. For the reddest stars, the relationships between the cross-correlation function and the stellar parameters (particularly $v \sin i$) are not valid (Santos et al. 2000, 2002), and those values are thus missing.

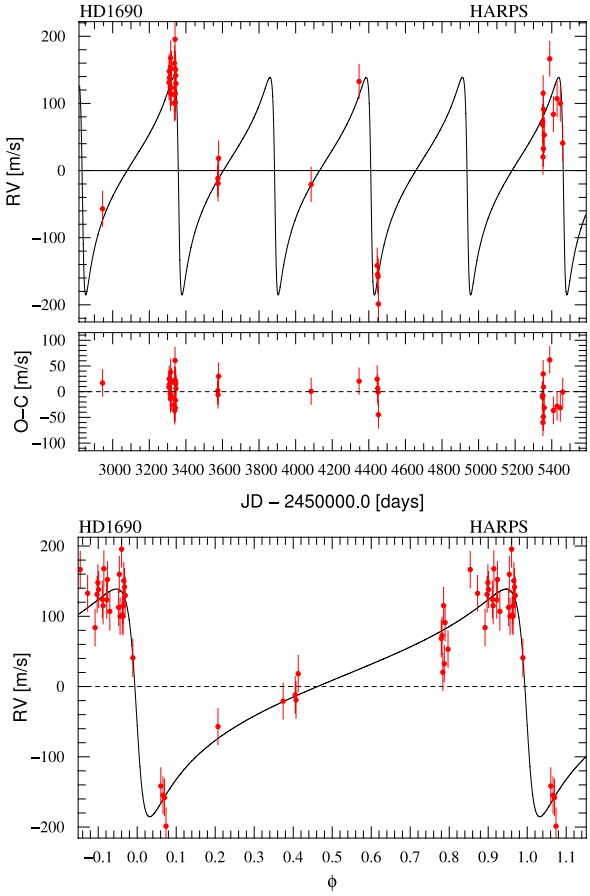

Fig. 1. *Top*: radial-velocity measurements of HD 1690 obtained with HARPS against time. The orbital fit is overplotted as a black line. The residuals to the fit are given below. *Bottom*: the phase-folded radial-velocity curve is shown. The best fit to the data is shown as a plain line.

3. Radial velocity data and proposed solutions

Radial-velocity time series of our sample stars have been obtained with the spectrograph HARPS (Mayor et al. 2003), mounted at the 3.60 m telescope in La Silla, ESO, Chile, mostly in the framework of the Guaranteed Time Observation programme (programme ID 072.C-0488), with additions from the follow-up volume-limited search programme 085.C-0019.

We used the HAM mode with a spectral resolving power of 115000, without simultaneous calibration of the velocity by the ThAr calibration lamp: the spectrograph is indeed stable enough for the precision of about 2 m/s targeted in this survey. Such a precision corresponds to a signal-to-noise ratio of 40 at 550 nm and to exposure times ranging from 2 to 15 min according to the stellar magnitude and external conditions, with a mean value of 8 min.

Each individual spectrum was then cross-correlated with a numerical mask, built from the stellar template better matching the stellar type, from M0 to F0 (Baranne et al. 1996). In addition to the position of the cross-correlation peak, the slope of the bisector line is measured on the stellar profile, indicating the level of photospheric activity that may affect the measurement of the peak position. The variation of the bisector span with the radial velocity is shown in Fig. 13 for all stars of the presented sample. Let us recall that an anti-correlation of the bisector span with respect to the peak position may depict a spot-related variation of the radial velocity, especially when the amplitudes of both variations are similar. Bisector variations may also be used to diagnose long term radial-velocity signals induced by variations in the stellar magnetic cycle (Santos et al. 2010a), as well as variations in the width of the cross-correlation function and temporal evolution of the activity tracer $\log R'_{\rm HK}$ (see Sect. 3.3).

In the time series of stellar radial velocities presented below, a significant variation was detected over periods usually longer than several hundreds days. After checking for activity indicators, we present an analysis of the results in terms of the planetary orbital signature except for two cases where the long-term activity cycle seems the dominant factor. In a few cases, several solutions are equivalent and more data over monthes to years are needed to conclude. Radial-velocity time series and the proposed solution are presented in Figs. 1 to 12. Individual measurements are available in electronic form at the CDS. Error bars for the derived parameters were estimated from a Monte-Carlo bootstrap analysis of the data sets using the routines of YORBIT (written by one of us, D.S.).

[1] See http://stev.oapd.inaf.it/

Table 1. Observed and inferred stellar parameters for the planet-hosting stars presented here.

Parameter		HD 1690	BD -114672	HD 25171	HD 33473A	HD 72659	HD 89839
Sp		K1III	K7V	F8V	G3V	G2V	F7V
V	[mag]	9.17	10.02	7.79	6.71	7.46	7.64
$B-V$	[mag]	1.354	1.263	0.554	0.662	0.612	0.523
π	[mas]	3.22 (1.43)	36.65 (1.73)	18.19 (0.45)	18.69 (0.49)	20.07 (0.75)	17.65 (0.55)
d	[pc]	310 (100)	27.3 (1.3)	55 (1.5)	53.5 (1.5)	49.8 (2)	57 (2)
M_V	[mag]	1.7 (0.7)	7.84 (0.1)	4.09 (0.07)	3.07 (0.06)	3.97 (0.1)	3.86 (0.07)
$B.C.$	[mag]	–0.75	–0.61	–0.03	–0.09	–0.06	–0.015
L	[$L_\odot$]	33.1	0.1	1.89	5.11	2.17	2.30
$T_{\rm eff}$	[K]	4393 (85)	4594 (134)	6160 (65)	5740 (62)	5926 (62)	6314 (65)
$\log g$	[cgs]	2.12 (0.17)	4.34 (0.31)	4.43 (0.1)	3.97 (0.1)	4.24 (0.1)	4.49 (0.12)
[Fe/H]	[dex]	–0.32 (0.06)	–0.47 (0.08)	–0.11(0.044)	–0.13 (0.04)	–0.02 (0.098)	+0.04 (0.043)
M_*	[$M_\odot$]	1.09 (0.15)	0.7 (0.1)	1.09 (0.03)	1.23 (0.03)	1.06 (0.04)	1.21 (0.03)
$v \sin i$	[km s^{-1}]	3.5	–	1.0	2.6	1.9	4.1
S_{MW}		0.11 (0.04)	0.75 (0.06)	0.15 (0.01)	0.15 (0.01)	0.16 (0.01)	0.15 (0.015)
$\log R'_{\rm HK}$	–	–	–	–4.99	–5.12	–4.97	–4.97
Age	[Gy]	6.7 (3.2)	4. (3.7)	4.0 (1.6)	4.4 (0.3)	6.5 (1.5)	1.2 (0.9)
R_*	[$R_\odot$]	16.7 (3.6)	0.7	1.18 (0.04)	2.23 (0.09)	1.36 (0.06)	1.25 (0.04)

Notes. For stars with lowest masses, the relationships which derive the activity index and projected velocity are not calibrated, and the flux in the blue calcium lines is too faint for an estimate of $\log R'_{\rm HK}$.

Table 1. continued.

Parameter		HD 113538	HD 167677	HD 217786	HIP 21934
Sp		K9V	G5V	F8V	K3
V	[mag]	9.02	7.90	7.80	9.9
$B-V$	[mag]	1.362	0.705	0.578	1.197
π	[mas]	63.03 (1.36)	17.29 (1.04)	18.23 (0.72)	28.77 (0.97)
d	[pc]	15.8 (0.4)	58 (3)	54.8 (2)	34.8 (1.2)
M_V	[mag]	8.03 (0.06)	4.08 (0.1)	4.11 (0.07)	7.19 (0.08)
$B.C.$	[mag]	–0.66	–0.135	–0.05	–0.62
L	[$L_\odot$]	0.09	2.09	1.89	0.19
$T_{\rm eff}$	[K]	4685 (155)	5474 (65)	5966 (65)	4674 (172)
$\log g$	[cgs]	4.28 (0.37)	4.43 (0.1)	4.35 (0.11)	4.2 (0.41)
[Fe/H]	[dex]	–0.17 (0.074)	–0.29 (0.043)	–0.135 (0.043)	+0.025 (0.12)
M_*	[$M_\odot$]	0.7 (0.1)	0.96 (0.02)	1.02 (0.03)	0.72 (0.02)
$v \sin i$	[km s^{-1}]	–	<1	1.4	–
$S_{\rm MW}$		1.05 (0.08)	0.17 (0.015)	0.15 (0.01)	0.57 (0.06)
$\log R'_{\rm HK}$	–	–	–4.99	–4.86	–4.86
Age	[Gy]	1.3 (1.3)	11 (1)	7.6	3.9 (3.8)
R_*	[$R_\odot$]	0.65 (0.1)	1.7 (0.1)	1.27 (0.06)	0.7 (0.1)

Table 2. Orbital and physical parameters for the planets presented in this paper.

Parameter		HD 1690 b	HD 25171 b	HD 72659 b	HD 217786 b
P	[days]	533 (1.7)	1845 (167)	3658 (32)	1319 (4)
T	[JD-2 400 000]	54 449 (5)	55 301 (449)	55 351 (59)	56 053 (7)
e		0.64 (0.04)	0.08 (0.06)	0.22 (0.03)	0.40 (0.05)
linear	[m/s/yr]	–7.2 (0.4)	–	–	–
γ	[km s^{-1}]	18.23 (0.03)	43.6 (0.01)	–18.15 (0.001)	9.98 (0.006)
ω	[deg]	122 (8)	96 (89)	–99.3 (6.5)	100 (2)
K	[m s^{-1}]	190 (29)	15.0 (3.6)	41.0 (1.3)	261 (20)
$a_1 \sin i$	[10^{-3} AU]	7.1 (1)	2.5 (0.3)	13.4 (0.4)	28.8 (1.5)
$f(m)$	[$10^{-9} M_\odot$]	181 (84)	0.66 (1.2)	24.2 (2.2)	1857 (307)
$m_2 \sin i$	[$M_{\rm Jup}$]	6.1 (0.9)	0.95 (0.10)	3.15 (0.14)	13.0 (0.8)
a	[AU]	1.3 (0.02)	3.02 (0.16)	4.74 (0.08)	2.38 (0.04)
$N_{\rm meas}$		42	24	50*a*	15
Span	[days]	2547	2314	4515	1538
σ (O–C)	[m s^{-1}]	29	3.4	4.2	2.5
$\chi^2_{\rm red}$		1.6	1.9	3.7	2.1

Notes. T is the epoch of periastron. σ (O–C) is the residual noise after orbital fitting of the combined set of measurements. *linear* is the slope of the observed drift with time.

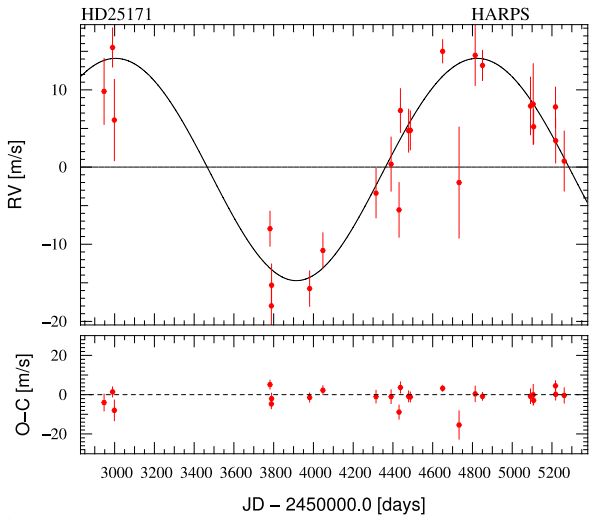

Fig. 2. Radial-velocity measurements of HD 25171 obtained with HARPS against time and the residuals to the best-fit model.

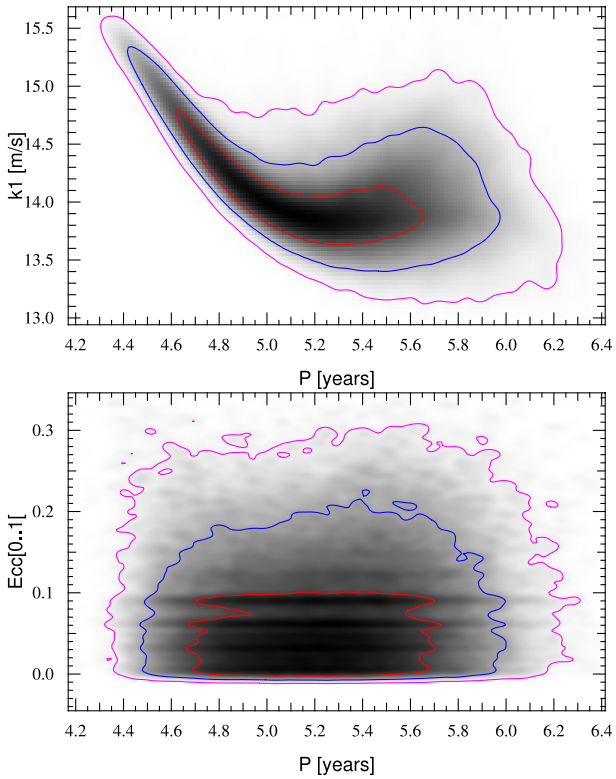

Fig. 3. Variations of χ^2 as a function of various related parameters of the fit for HD 25171, using Markov-chain simulations. (*Top*) Correlation plot between the orbital period and radial-velocity semi-amplitude. (*Bottom*) Correlation plot between eccentricity and orbital period. The lines show 1, 2 and 3-σ iso-contour plots.

3.1. Complete orbits

HD 1690

Fourty-two HARPS measurements of the giant star HD 1690 were gathered from November 2003 to October 2010, as shown in Fig. 1. The presence of a few giant stars in the HARPS volume-limited sample is due to a revision of the parallax from the original Hipparcos output catalogue (ESA 1997) to the new estimates of parallaxes from van Leeuwen (2007). For star HD 1690, the parallax was revised from 43.42 to 3.22 mas.

The average formal accuracy of individual data points is 1.8 m/s. Variations of the radial velocity have a standard deviation of 110 m/s, while the bisector slope varies with a standard deviation of less than 20 m/s.

When the variation of the stellar radial velocity of HD 1690 is interpreted in terms of a Keplerian orbit of a planet, the best solution corresponds to a 532 day period. The residual scatter of the fit is rms = 25.3 m/s. Since the parent star is a giant, one expects the residual scatter to originate from high-frequency stellar oscillations, with an amplitude that is standard for red giants (Sato et al. 2005). No significant period is found in the residual of the fit, which is also compatible with the common behaviour of radial-velocity oscillation signatures in giants (Hatzes et al. 2007). In order to better reflect the actual velocity jitter and to get a reduced χ^2 closer to 1, we quadratically added 25 m/s to the individual errors. This jitter amplitude is common for a K giant with $B - V = 1.35$, a range where it may vary from 20 to 100 m/s (Frink et al. 2001). The residuals show a slight negative slope, indicating a possible distant companion. The solution implying a linear drift reproduces the data better than the single planet with a probability of 75% (F-test of Pourbaix & Arenou (2001)). The orbit of the planet shows large eccentricity, $e = 0.64$, leading to a minimum mass of the companion of about 6 $M_{\rm Jup}$. Figure 1 shows the phase-folded data points and best-fit orbit. It must be noted that the solution shown in this analysis is not very robust: the removal of ∼12 data points significantly changes the period of the best-fit. The reason for this are several peaks of equivalent power in the periodogram. The presented solution is found by performing 10 000 Monte Carlo simulations and including all data points. The complete solution is given in Table 2. It is possible that further observations modify the solution proposed here, or increase the number of planets in the system.

HD 25171

The non-active star HD 25171 was observed 24 times with HARPS between November 2003 and March 2010 with average errors of 3 m/s. A long-period variation is detected and attributed to the presence of a distant Jupiter-like planet. The standard deviation of the velocity drops by a factor 3 when a best-fit Keplerian orbit is removed from the data. A period of 5 years is found, corresponding to a planet minimum mass of 0.95 $M_{\rm Jup}$ (Fig. 2). Since the semi-amplitude is low and the long orbit only partially covered by observations, we performed a Monte-Carlo Markov-chain analysis to support the detection. The most relevant output plots are shown on Fig. 3: the χ^2 distribution of the fit, against related parameters such as the semi-amplitude, the eccentricity, and the orbital period. The correlation plots show that several equivalent solutions exist, but in a limited range of these parameters The complete solution is given in Table 2 from the bootstrap analysis that gives more conservative errors than the MCMC analysis. The scatter of the residuals to this fit is 3.4 m/s, which is of the order of individual measurements.

HD 72659

A total of 36 spectra of HD 72659 have been gathered between February 2004 and June 2010, with an average error of 2.3 m/s (Fig. 4, red points). The radial-velocity time series shows variations with a maximum amplitude of 70 m/s, whereas the bisector

Table 3. Orbital and physical parameters for HD 113538 b and c[1].

Parameter		HD 113538 b	HD 113538 c
P	[days]	263.3 (2.3)	1657 (48)
T	[JD-2 400 000]	54 950 (8.5)	56 110 (515)
e		0.61 (0.11)	0.32 (0.06)
ω	[deg]	74 (20)	–90 (21)
K	[m s^{-1}]	15.5 (12)	16.5 (1.4)
$a_1 \sin i$	[10^{-3} AU]	0.26 (0.07)	2.36 (0.15)
$f(m)$	[10^{-9} $M_\odot$]	0.048 (0.10)	0.65 (0.14)
$m_2 \sin i$	[$M_{\rm Jup}$]	0.27 (0.08)	0.71 (0.06)
a	[AU]	0.71 (0.01)	2.43 (0.06)
γ	[km s^{-1}]	39.23 (0.012)	
$N_{\rm meas}$		29	
Span	[days]	2268	
σ (O – C)	[m s^{-1}]	1.8	
$\chi^2_{\rm red}$		1.5	

Notes. Note that there is a marginal possibility for the radial velocity series of this star to be caused by activity rather than planetary signatures (see text).

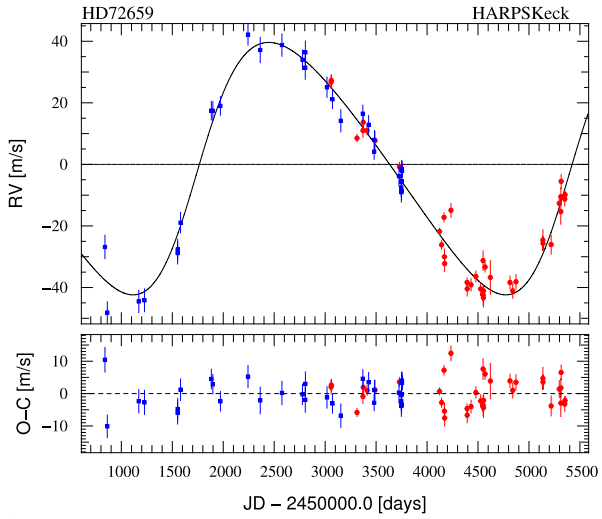

Fig. 4. Radial-velocity measurements of HD 72659 obtained with HARPS (red points) and Keck (blue points) against time, together with the best-fit solution of the combined data sets and the residuals.

slope is stable to 6 m/s. The full period is seemingly not covered by our observations. The low activity of the star and the absence of a correlation of the bisector span or activity tracers with the radial velocity exclude the possibility that activity alone explains the velocity variation.

A planetary companion has already been reported by Butler et al. (2003) in this system, with poor constraint on the orbit. A refined solution is published in Butler et al. (2006). The combination of both Keck/HIRES and HARPS data reinforces the solution with more than 12 year span and in particular, the orbital period is now well determined. The offset between the Keck and HARPS data sets is left as a free parameter to the fit. Our solution is compatible with the one given in Butler et al. (2006), but with an error on the period seven times smaller. The best-fit solution shows the presence of a single orbiting 3.1-$M_{\rm Jup}$ planet in a slightly eccentric orbit of period 3658 days (Fig. 4). The residuals of the fit have a standard deviation of 3.7 m/s. No long-term trend or significant peak in the periodogram of residuals is found to explain this low-amplitude extra jitter. The complete solution is given in Table 2.

HD 113538

We secured 29 HARPS measurements of star HD 113538 between February 2004 and June 2010; they have average errors of 1.8 m/s. The radial velocity variations have a peak-to-peak amplitude of 50 m/s over the 2268 day time span of the observations, and they do not correlate with the bisector span variations. The best-fit solution involves a single planet with a long period and very eccentric orbit, but residuals to the fit are large with regard to individual errors (standard deviation of 5.4 m/s), and with a poorly defined semi-amplitude. A better solution is depicted with a two-Keplerian orbit model, involving a Jupiter-like planet in a slightly eccentric orbit of 1657 day period, plus a Saturn-like planet in a shorter eccentric orbit of 263 days. Then the residuals to the combined fit drop to 1.8 m/s. The complete solution is given in Table 3 and Fig. 5. Simulations were performed to confirm that the two-planet solution is statistically more significant than the single planet + long-term trend variation: the data are permuted around the one-planet solution, and the residuals are statistically compared with the two-planet model residuals. The probability that the two-planet model suits the data better is obtained by calculating the number of realisations where the χ^2 obtained with the permuted data is smaller than with real data. The use of the genetic algorithm in this iterative process allows more reliability than false alarm probability tests on the periodogram.

As an additionnal test and because the star is significantly active, we used the activity indicators to check whether the signal is caused by activity. The FWHM of the cross-correlation function shows a moderate correlation to the Mount Wilson S activity index, which is based on calcium emission, with a correlation coefficient of 60%. Our previous analysis shows that the two-planet model is statistically robust, but we remain cautious because stellar activity probably affects the solution.

HD 217786

Fifteen spectra of HD 217786 were acquired from July 2006 to October 2009. They show very large velocity variations, with a peak-to-peak amplitude of 390 m/s when individual errors are 2.1 m/s on average. The bisector span shows small variations that are not correlated with the radial velocity, the FWHM and the calcium activity index are not correlated, and the star is not active with $\log R'_{\rm HK}$ of –4.86. The velocity variation is thus not caused by activity. A Keplerian solution with a 1320 day period, 0.4 eccentricity and 260 m/s semi-amplitude is the best-fit solution to the data set (Fig. 6). The residuals to the fit have an rms of 2.5 m/s. In order to further increase the significance of the fit, additional observations around periastron and apastron would be necessary. The minimum mass of the orbiting planet is 13 $M_{\rm Jup}$, within the overlapping region between giant planets and brown dwarfs. The complete solution is given in Table 2.

3.2. Incomplete orbits

HD 33473A

Twenty-six HARPS spectra of HD 33473A were collected from October 2003 to March 2010 with an average error of 1.9 m/s. Large amplitude variations of the velocity have a standard deviation of 200 m/s. A velocity variation caused by stellar activity is rejected by our data, because the bisector span is constant. The 2300-day time span covered by our observations is not long enough to distinguish between two solutions: an uncomplete, single orbit with an ill-constrained period (16 to 38 years), or

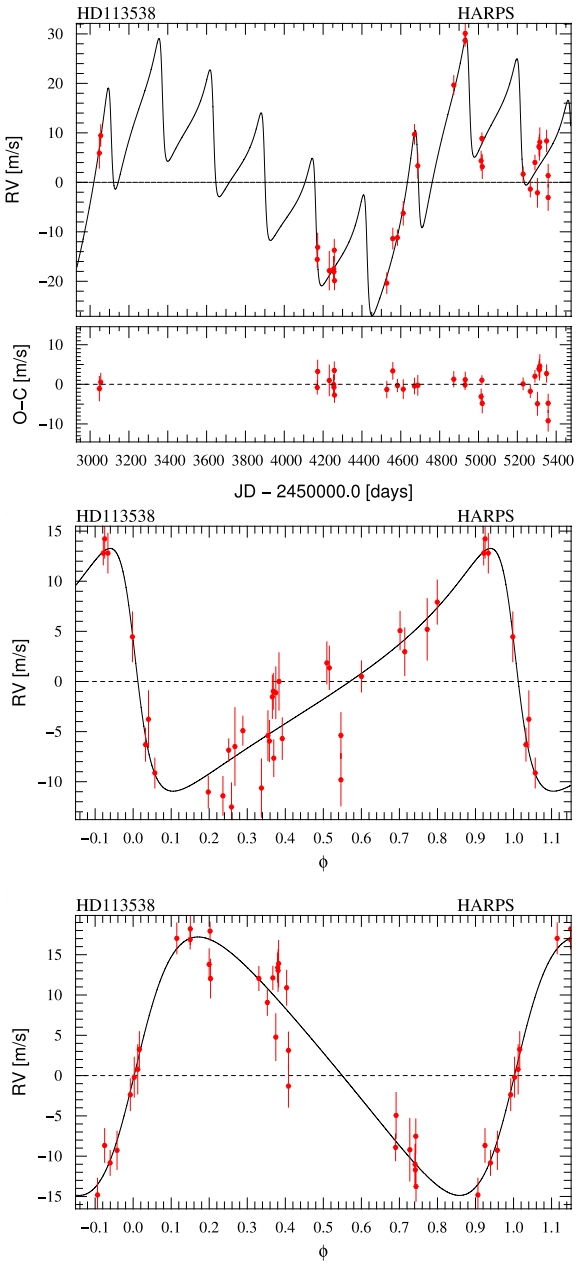

Fig. 5. Radial-velocity measurements of HD 113538 obtained with HARPS against time, and for both planets, against their orbital phase.

a ~2800 day period orbit with a longer-term drift. Both solutions give a similar χ^2. In another year, with continuing observations of this system, we should be able to better constrain the system, because then the shorter period will be entirely observed. With such a difference in the derived period, the mass of the companion is evidently very uncertain, ranging from 6 to 29 $M_{\rm Jup}$. However, HD 33473A has a known visual companion, HD 33473B, with an angular separation of 10 arcsec and magnitude difference 3.4 in the optical. It is thus a K8-like star at 500 UA distance, at least, which corresponds to a period longer than 10^4 years. The existence of this distant stellar companion strongly reinforces the justification of a planet model involving a long-term drift. This is the solution presented in this paper (Table 4 and Fig. 7). It gives an O–C residual scatter of about 2.4 m/s.

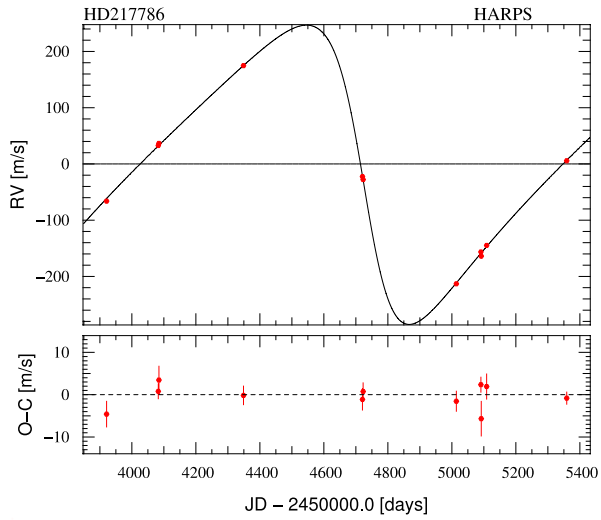

Fig. 6. Radial-velocity measurements of HD 217786 obtained with HARPS against time.

HD 89839

From February 2004 to June 2010, 39 measurements of the low-activity star HD 89839 were recorded. They show long-term radial-velocity variations with a peak-to-peak amplitude of 90 m/s (Fig. 8). No correlation is found between the bisector and the velocity, excluding the stellar activity as the origin of the observed signal. Although the orbit is not regularly sampled by the observations, a period of 9.5 to 27 years days emerges, with some excentricity. As we are entering the descending section of the radial velocity curve, this solution will be confirmed and refined within the next four years. The current solution gives a semi-amplitude variation of 45 m/s, corresponding to a 3.9 $M_{\rm Jup}$ planet. The standard deviation of the residuals to the fit is 3.9 m/s, similar to the average error bar of the measurements. The MCMC output distributions show the correlated behaviour of eccentricity, semi-amplitude, and orbital period in Fig. 9.

HD 167677

Twenty-six HARPS measurements of HD 167677 were collected between May 2005 and October 2010, with an average 1σ error of 1.6 m/s. They show radial-velocity fluctuations at the level of 15 m/s standard deviation, and with a periodicity of about 1800 days. The activity indicator $\log R'_{\rm HK}$ is typical of a non-active star (–4.99). The bisector span and FWHM of the cross-correlation function do not vary in phase with the calcium index or the velocity. So the interpretation in terms of pure stellar activity is excluded. The best-fit Keplerian solution corresponds to a planet with minimum mass 1.36 $M_{\rm Jup}$ in a slightly eccentric orbit, as shown in Fig. 10. The residuals to the fit have a standard deviation of 2.6 m/s. The MCMC analysis allowed us to quantify the correlation between the orbital parameters, and Fig. 11 shows the relation between eccentricity, period, and semi-amplitude. Additionnal data would be needed to get more precise parameters of the orbit, and can be collected in the next years. The complete solution is given in Table 4.

Table 4. Orbital and physical parameters for the companions with incomplete orbits.

Parameter		HD 33473A b	HD 89839 b	HD 167677 b
P	[days]	2798 (60)	6601(–3570, +4141)	1814 (100)
T	[JD-2 400 000]	55 053 (93)	60 067 (–4954, +4425))	55 656 (123)
e		0.07 (0.01)	0.32 (0.2)	0.17 (0.07)
linear	[m/s/yr]	–78.9 (0.07)	–	–
γ	[km s^{-1}]	44.2 (0.001)	31.7 (0.002)	–57.24 (0.01)
ω	[deg]	141 (15)	–22 (144)	–80 (24)
K	[m s^{-1}]	91 (1.1)	45.5 (2.3)	23.7 (3)
$a_1 \sin i$	[10^{-3} AU]	23.4 (0.7)	22 (17)	3.9 (0.4)
$f(m)$	[$10^{-9} M_\odot$]	218 (12)	38 (10)	2.4 (2.3)
$m_2 \sin i$	[$M_{\rm Jup}$]	7.2 (0.3)	3.9 (0.4)	1.36 (0.12)
a	[AU]	4.17 (0.09)	6.8 (–2.4, +3.3)	2.9 (0.12)
$N_{\rm meas}$		26	39	26
Span	[days]	2465	2297	1977
σ (O–C)	[m s^{-1}]	2.4	3.0	2.6
$\chi^2_{\rm red}$		3.5	1.9	3.1

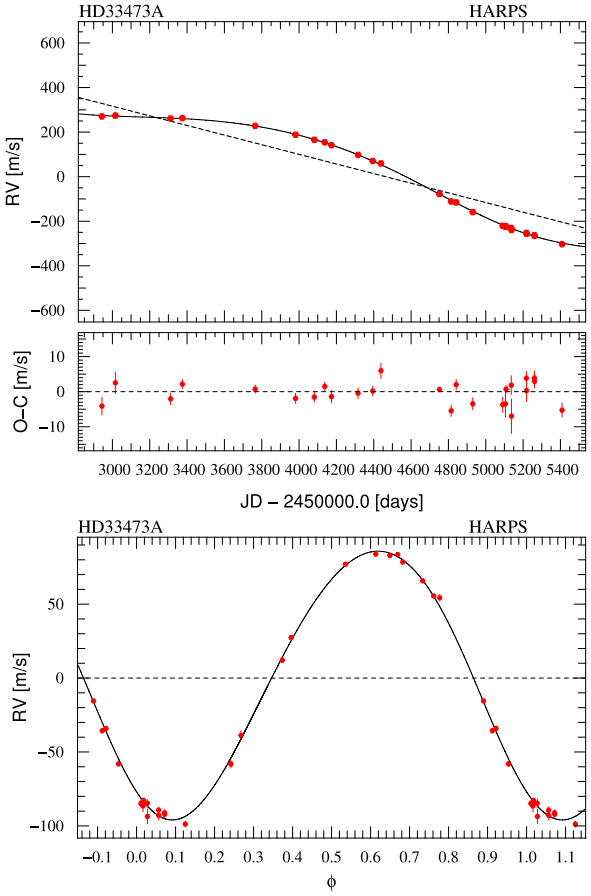

Fig. 7. Radial-velocity measurements of HD 33473A obtained with HARPS against time (*Top*) and phase (*Bottom*).

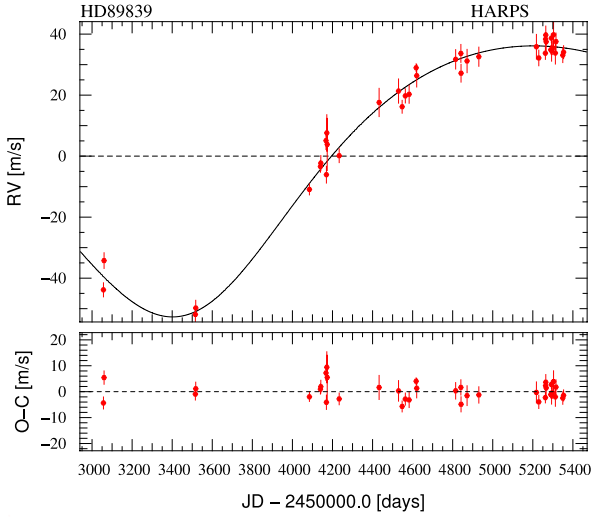

Fig. 8. Radial-velocity measurements of HD 89839 obtained with HARPS against time.

3.3. Long-period planets or magnetic cycles?

BD -114672

Nineteen HARPS measurements were obtained of star BD -114672 between July 2005 and June 2010, with an average error of 1.9 m/s (Fig. 12). A peak-to-peak velocity variation of 28 m/s is observed. The bisector slope shows a significant degree of anti-correlation (Fig. 13), and a visible reversal in the core of the calcium lines confirms that the star is active. However, the main radial-velocity variation has a significant peak of periodicity at 1692 days, much too long for a rotation period, and no significant peak in the range 5–50 days. An attempt has been made to correct for the activity as in Melo et al. (2007) and Boisse et al. (2009) by linearly fitting the bisector-velocity correlation and subtracting this trend from the velocity measurements. The resulting solution is not significantly different. In addition, Fig. 14 shows a significant degree of correlation between the full-width-at-half maximum of the cross-correlation function, and the calcium activity index (Mount Wilson S value). The stellar lines therefore appear distorted with a long timescale. This behaviour may indicate a velocity variation owing to a slow evolution of the stellar activity, rather than a long-period planetary companion. Both interpretations are possible however, because the degree of correlation as shown in Fig. 14 is not high (72%).

When we fit the data in search for a Keplerian orbit, we find a circular orbit of a planet with a minimum mass of 0.6 $M_{\rm Jup}$ and 2.5 AU semi-major axis. It corresponds to a signal at a period of 1500 to 1900 d, or 4 to 5 years. This is compatible with the typical duration of an activity cycle, although on the short end (see e.g. Baliunas et al. 1995; Fares et al. 2009; Metcalfe et al. 2010).

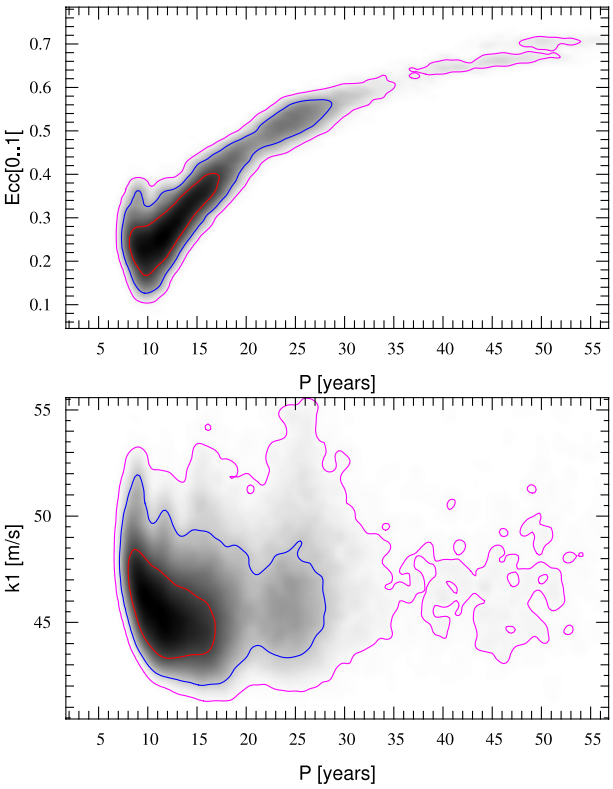

Fig. 9. Statistical tests on the RV time series of HD 89839: (*top*) correlation plot between period and eccentricity; (*bottom*) correlation plot between velocity semi-amplitude and period.

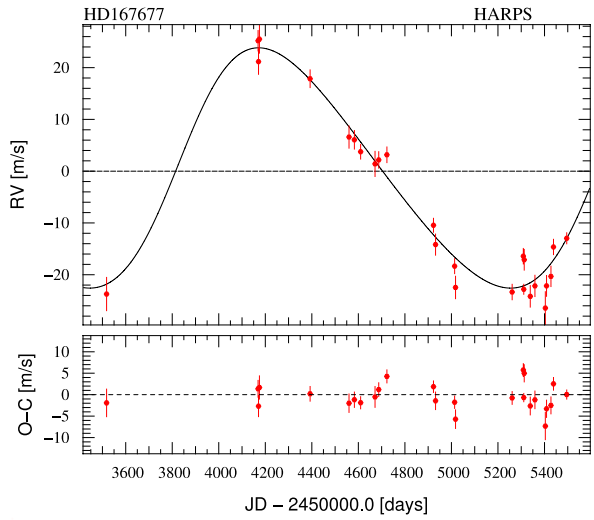

Fig. 10. Radial-velocity measurements of HD 167677 obtained with HARPS against time.

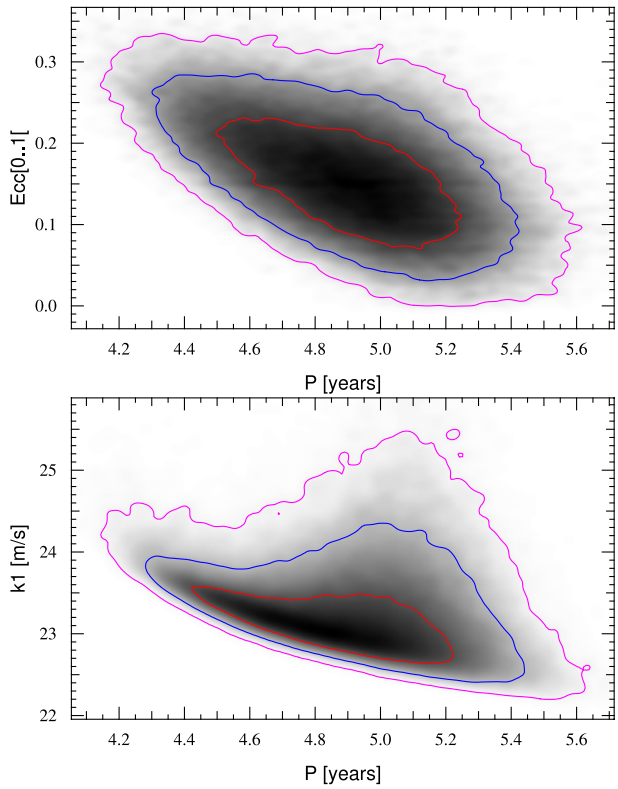

Fig. 11. Statistical tests on the RV time series of HD 167677: (*top*) correlation plot between period and eccentricity; (*bottom*) correlation plot between velocity semi-amplitude and period.

HIP 21934

Twenty-three spectra of HIP 21934 were secured with HARPS from January 2004 to April 2010, with an average error of 1.4 m/s. Low-amplitude velocity variations are detected, with clearly a long period variation and an additional short-period component (Fig. 12). However, as for BD -11467, the full-width-at-half maximum of the cross-correlation function is correlated to the activity index, with a coefficient of 89% (Fig. 14). This again indicates that the velocity variation may be caused by pure stellar activity fluctuations, with a slowly evolving distortion of stellar lines over several years. In this case, the correlation is stronger, and the interpretation in terms of magnetic cycle is favoured, although the star is moderately active during most of the cycle. The velocity variation of this cycle mimics the signature of a long-period (1100 days) planetary companion of minimum mass less than one Jupiter mass. This result is worse than expected in dedicated studies by Santos et al. (2010a), because the amplitude of the effect is higher – even though HIP 21934 is a K dwarf, as was considered in this study. It illustrates the importance of monitoring and considering activity tracers simultaneously to radial velocities for a valid interpretation of the results of planet search surveys, especially when low-velocity amplitudes and long orbital periods are considered. The length of the magnetic cycle, if confirmed as such, is 3–3.5 years, again a rather short period compared with the sample of Baliunas et al. (1995). This would correspond to a ~7-yr magnetic cycle, intermediate between the 2-yr cycle of τBoo (Fares et al. 2009) and 22-yr cycle of the Sun.

4. Conclusion

We presented the observational material secured with the high-precision radial-velocity spectrograph HARPS on ten stars in search for the signature of planetary systems. One star, HD 7265, had a published planet, for which we could refine the mass determination and orbital elements. Figure 15 shows how these new planets hold on the total distribution of mass, period, and eccentricity of known exoplanets.

After the first seven years of our survey, we aim at giving first synthetic views of the results by publishing our

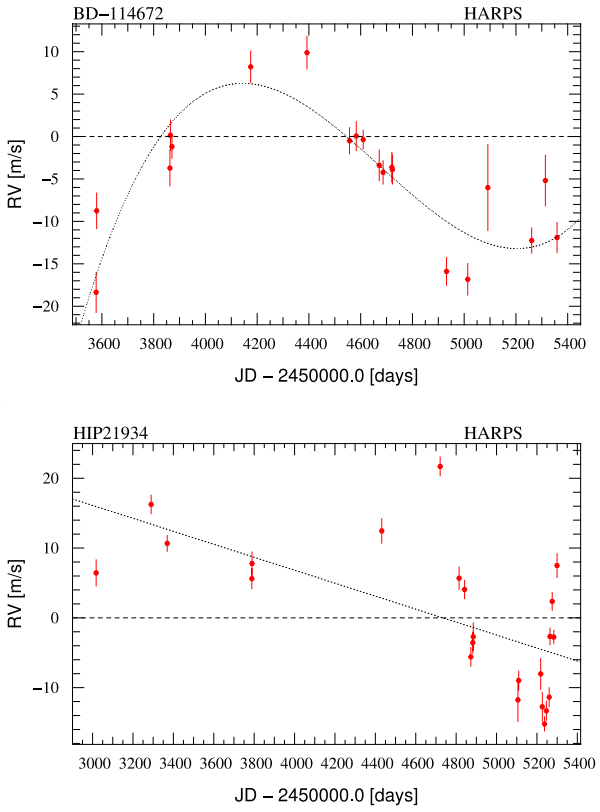

Fig. 12. Radial-velocity measurements against time of stars BD -114672 and HIP 21934 for which the long-term velocity variation is interpreted as caused by the magnetic activity cycle of the star.

current detections of long period companions in the planetary mass regime. The radial-velocities time series reported in this work sometimes appear incomplete, and several different solutions cannot be distinguished, as illustrated for some cases by our χ^2 distributions against related parameters P, K and e. Measurements are continuing however, and in a few years we will be able to better constrain the orbits and refine mass determination of the depicted systems. The discovered companions are giant planets and one or two brown dwarfs, with orbital periods more than three years. In two cases, indications of velocity variations caused by stellar long-term activity evolution are shown, rather than planetary signatures.

Finding long-period, massive planets in volume-limited surveys is of prime importance to get the complete picture of extrasolar system's architecture, despite the natural biases towards short-period planets of the radial-velocity method. However, when searching for best-fit solutions of planetary orbits with periods larger than the time span of the observations, one meets the degeneracy of several types of solutions, with or without linear drifts, additional components in the system, or accounting for degeneracies in the fitted parameters. One expects long period planets to be part of systems, because inward migration should not have blown out the inner planets, and series of giant planets may exist as in the solar system. Orbital fitting for long-period planets is thus more uncertain than for shorter-period planets. The significance of periods, masses, and eccentricities of known radial-velocity long-distance planets should then be taken with some care, as the best-fit solution is likely to evolve when more data are available. One recent example of revisiting radial-velocity solutions of long-period planets of 47 UMa is illustrated by Gregory & Fischer (2010). The solutions given in the present work will also be more constrained with additional data, either to complete a period, or to confirm the presence of an additional component in the system. The data are still being collected with HARPS under the observing programme 085.C-0019 (P.I. Lo Curto) and will be presented and analysed in forthcoming papers.

Direct imaging of the new planetary systems whose discovery is reported here will be possible, especially for the most nearby target HD 113538. The angular separation presently expected for their planets is 0.152 arcsec from its stars.

As for other planets around giant stars, HD 1690 b is a massive gaseous planet, similar to the recently discovered HD 32518 b (Döllinger et al. 2009). There are now about 20 known planetary systems to giant stars, all with semi-major axes exceeding 0.59 AU and minimum masses larger than 1.5 $M_{\rm Jup}$. This narrower spread of parameters of planets around giant stars than around main-sequence stars may be explained by the high residual velocity caused by radial oscillations. With periods of hours to days and amplitude of several tens of m/s (Hatzes et al. 2007), these intrinsic variations of the star increase the difficulty of detecting the low-mass end of the planets. Regarding arguments such as the filling of the Roche lobe by the primary, the minimum period expected for a giant of 1.09 $M_{\odot}$ mass as HD 1690 is about 200 days (Mermilliod & Mayor 1996), which is below the observed 532 day orbit.

It may be a new fact that magnetic cycles of stars may have a signature on the radial-velocity behaviour over long timescales, with amplitudes similar to the gravitational perturbation of a giant planet in a large-distance orbit. This was recently discarded by Santos et al. (2010a) for a limited sample of G and early K stars, and is further discussed by Lovis et al. (in prep.). Two examples are given here, of stars from the volume-limited sample followed-up by HARPS (HIP 21934 and BD -114672) showing the width of stellar lines affected by the long-term magnetic cycle rather than affected by a distant planetary companion. In this paper, we tentatively interpret the radial-velocity variations as caused by this long-term cycle, but investigations should be continued in this field, from analyses of a larger sample and from simulations.

One planetary system is presented around HD 113538 with a Saturne-Jupiter-like pair of planets at 0.7 and 2.4 AU respectively. Like the vast majority of planet pairs in systems, the most massive planet is the outer planet. This is possibly a detection bias towards the long periods, because the signal amplitude greatly decreases with star-planet distance.

Interestingly, most of the planet host stars discussed here are metal-poor, contradicting the usual conclusion that stars with giant planets are usually more metal-rich than the average field dwarfs (e.g. Santos et al. 2004; Fischer & Valenti 2005). In a recent paper, Santos et al. (2010b) have also discovered three giant planets orbiting metal-poor stars from the HARPS survey, all in long period orbits. Similarly, it has been noted that the metallicity distribution of giant stars hosting planets does not favour metal-rich stars (Pasquini et al. 2007). Though preliminary, these facts suggest that long period giant planets are not uncommon around low-metallicity stars, as shown by a dozen other examples (see `http://exoplanet.eu/catalog.php`). This possible trend will be confirmed by this continuing survey and others.

Finally, let us stress that discoveries of giant planets in very long orbits is only beginning, because of the long baselines that are needed. When the star activity is not an issue, Jupiter twins will be soon collected by radial-velocity surveys, and such systems will be good candidates when searching for Earth twins.

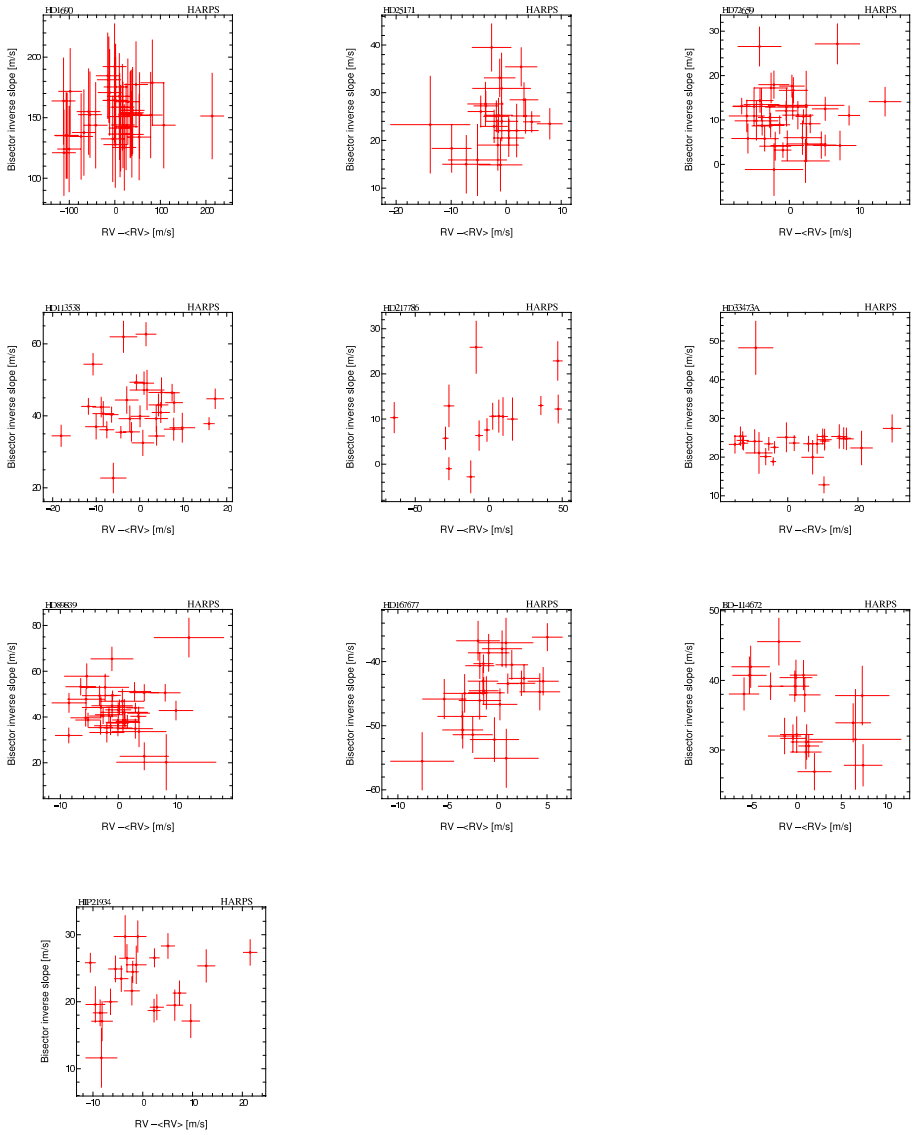

Fig. 13. Bisector slope variations with respect to radial velocity for all data sets.

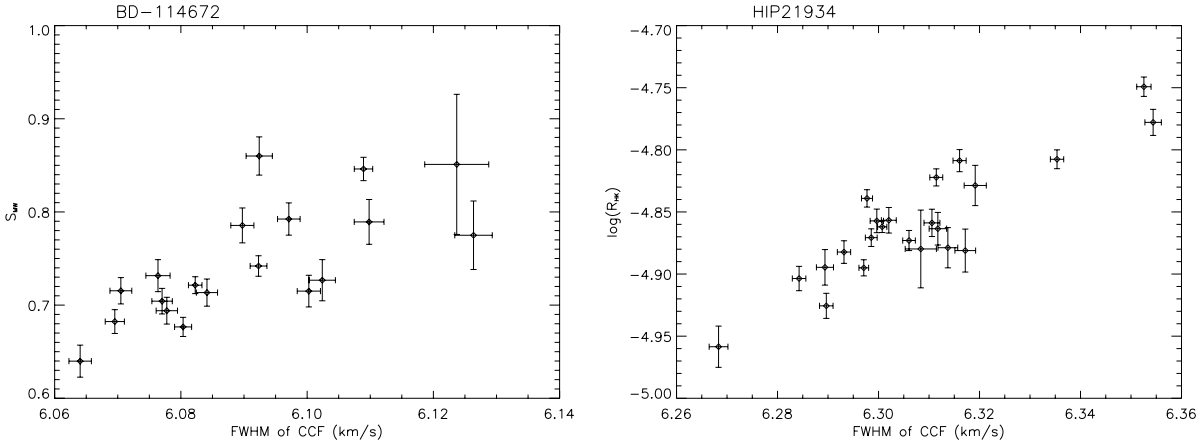

Fig. 14. Variations of the activity tracer, $\log R'_{\rm HK}$ or Mount-Wilson S index, are correlated to the full-width-at-half maximum of the cross-correlation function of stars BD -114672 (*Left*) and HIP 21934 (*Right*). This indicates that the long-term velocity variation is probably caused by the magnetic cycle of the star, rather than a long-period planetary companion. The correlation is more significant for star HIP 21934.

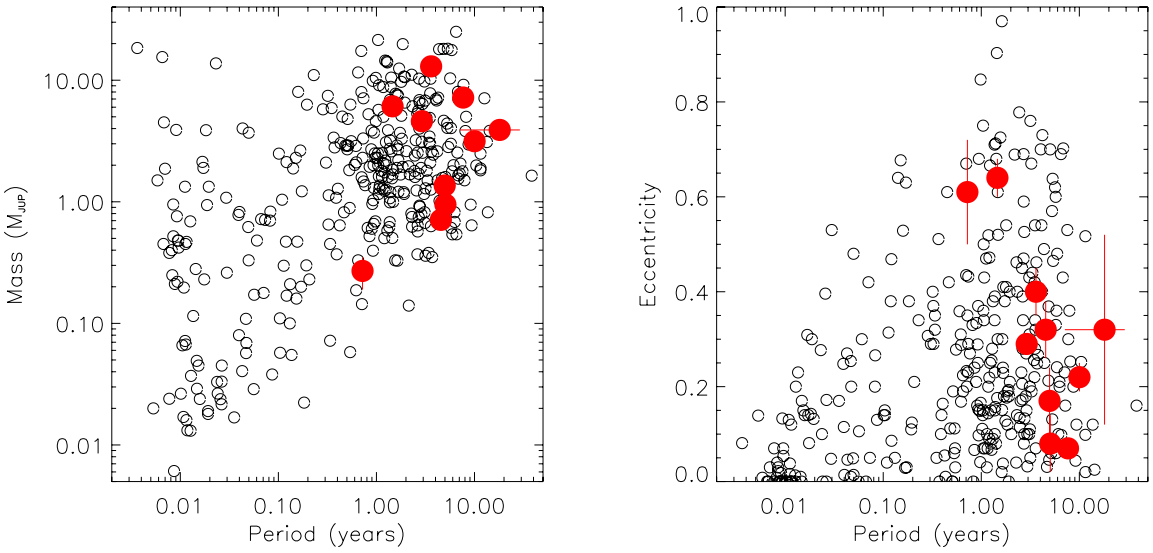

Fig. 15. Mass-period and period-eccentricity diagrams. Open circles show the full sample of radial-velocity planets, as of July 2010, and the filled circles depict the planets described here.

The role of Jupiter-like planets in the formation of habitable planets is important (Raymond 2006). Finding the most massive planet in a system, on a distant orbit, may thus be a first step to discovering planetary systems similar to the solar system, and searching for Earth analogs.

Acknowledgements. N.C.S. would like to thank the support by the European Research Council/European Community under the FP7 through a Starting Grant, as well from Fundacao para a Ciência e a Tecnologia (FCT), Portugal, through a contract funded by FCT/MCTES (Portugal) and POPH/FSE (EC), and in the form of grants reference PTDC/CTE-AST/098528/2008 and PTDC/CTE-AST/098604/2008. We are grateful to the ESO staff for their support during observations. Thanks are owing to the anonymous referee for her/his good comments and suggestions to improve the paper.

References

Baliunas, S. L., Donahue, R. A., Soon, W. H., et al. 1995, ApJ, 438, 269
Baraffe, I., Chabrier, G., Barman, T. S., Allard, F., & Hauschildt, P. H. 2003, A&A, 402, 701
Baranne, A., Queloz, D., Mayor, M., et al. 1996, A&AS, 119, 373
Boisse, I., Moutou, C., Vidal-Madjar, A., et al. 2009, A&A, 495, 959
Butler, R. P., Marcy, G. W., Vogt, S. S., et al. 2003, ApJ, 582, 455
Butler, R. P., Wright, J. T., Marcy, G. W., et al. 2006, ApJ, 646, 505
Casagrande, L., Portinari, L., & Flynn, C. 2006, MNRAS, 373, 13
da Silva, L., Girardi, L., Pasquini, L., et al. 2006, A&A, 458, 609
Döllinger, M. P., Hatzes, A. P., Pasquini, L., Guenther, E. W., & Hartmann, M. 2009, A&A, 505, 1311
ESA 1997, VizieR Online Data Catalog, 1239, 0
Fares, R., Donati, J., Moutou, C., et al. 2009, MNRAS, 398, 1383
Fischer, D. A., & Valenti, J. 2005, ApJ, 622, 1102
Flower, P. J. 1996, ApJ, 469, 355
Fortney, J. J., Marley, M. S., Saumon, D., & Lodders, K. 2008, ApJ, 683, 1104
Frink, S., Quirrenbach, A., Fischer, D., Röser, S., & Schilbach, E. 2001, PASP, 113, 173
Gregory, P. C., & Fischer, D. A. 2010, MNRAS, 403, 731
Hatzes, A. P., Döllinger, M. P., & Endl, M. 2007, Commun. Asteroseismol., 150, 115
Kurucz, R. 1993, ATLAS9 Stellar Atmosphere Programs and 2 km s^{-1} grid, Kurucz CD-ROM No. 13 (Cambridge, Mass.: Smithsonian Astrophysical Observatory)
Lo Curto, G., Mayor, M., Clausen, J. V., et al. 2006, A&A, 451, 345
Lo Curto, G., Mayor, M., Benz, W., et al. 2010, A&A, 512, A48
Mayor, M., Pepe, F., Queloz, D., et al. 2003, The Messenger, 114, 20
Melo, C., Santos, N. C., Gieren, W., et al. 2007, A&A, 467, 721
Mermilliod, J., & Mayor, M. 1996, in Cool Stars, Stellar Systems, and the Sun, ed. R. Pallavicini, & A. K. Dupree, ASP Conf. Ser., 109, 373
Metcalfe, T. S., Basu, S., Henry, T. J., et al. 2010, ApJ, 723, L213
Moutou, C., Mayor, M., Bouchy, F., et al. 2005, A&A, 439, 367
Moutou, C., Mayor, M., Lo Curto, G., et al. 2009, A&A, 496, 513
Naef, D., Mayor, M., Benz, W., et al. 2007, A&A, 470, 721
Naef, D., Mayor, M., Lo Curto, G., et al. 2010, A&A, 523, A15
Pasquini, L., Döllinger, M. P., Weiss, A., et al. 2007, A&A, 473, 979
Pepe, F., Mayor, M., Queloz, D., et al. 2004, A&A, 423, 385
Pourbaix, D., & Arenou, F. 2001, A&A, 372, 935
Raymond, S. N. 2006, ApJ, 643, L131
Ségransan, D., Mayor, M., Udry, S., et al. 2010, A&A, submitted
Santos, N. C., Mayor, M., Naef, D., et al. 2000, A&A, 361, 265
Santos, N. C., Mayor, M., Naef, D., et al. 2002, A&A, 392, 215
Santos, N. C., Israelian, G., & Mayor, M. 2004, A&A, 415, 1153
Santos, N. C., Gomes da Silva, J., Lovis, C., & Melo, C. 2010a, A&A, 511, A54
Santos, N. C., Mayor, M., Benz, W., et al. 2010b, A&A, 512, A47
Sato, B., Kambe, E., Takeda, Y., et al. 2005, PASJ, 57, 97
Sneden, C. 1973, Ph.D. Thesis, Univ. of Texas
Sousa, S. G., Santos, N. C., Israelian, G., Mayor, M., & Monteiro, M. J. P. F. G. 2007, A&A, 469, 783
Sousa, S. G., Santos, N. C., Mayor, M., et al. 2008, A&A, 487, 373
van Leeuwen, F. 2007, A&A, 474, 653